Acta Crystallographica Section D
Biological Crystallography
ISSN 0907-4449

Rhombohedral crystals of *Mycobacterium tuberculosis* phosphopantetheine adenylyltransferase

Kathrin L. Brown, Van K. Morris and Tina Izard*

Department of Hematology–Oncology, St Jude Children's Research Hospital, Memphis, Tennessee 38105, USA

Correspondence e-mail: tina.izard@stjude.org

Received 15 October 2003
Accepted 11 November 2003

The penultimate step of prokaryotic coenzyme A (CoA) biosynthesis is directed by the essential enzyme phosphopantetheine adenylyltransferase (PPAT; EC 2.7.7.3), an attractive target for antibiotics. The reaction catalyzed by PPAT is rate-limiting and involves the transfer of an adenylyl group from ATP to 4′-phosphopantetheine to form 3′-dephospho-CoA. Rhombohedral crystals of PPAT from *Mycobacterium tuberculosis* (Rv2965c) were obtained. The crystals belong to space group *R*32, with unit-cell parameters $a = 68.69$ Å, $\alpha = 91.81^\circ$. The crystals diffract to better than 2 Å resolution on a Cu $K\alpha$ rotating-anode generator. The packing density for one polypeptide chain in the asymmetric unit is 2.89 Å^3 Da^{-1}, with a solvent content of 0.57.

1. Introduction

Coenzyme A (CoA) is the major acyl carrier for all organisms and is obligatory for cell survival. CoA is an essential cofactor for over 4% of all cellular enzymes and is required for numerous synthetic and degradative reactions in intermediary metabolism (Robinshaw & Neely, 1985). CoA is synthesized in a series of five enzymatic steps from pantothenate (vitamin B_5), cysteine and ATP (Abkido, 1967). Firstly, pantothenate is phosphorylated by pantothenate kinase to generate 4′-phosphopantothenate. Secondly, cysteine is added by phosphopantothenoylcysteine synthase and its product is decarboxylated by pantothenoylcysteine decarboxylase to form 4′-phosphopantetheine. Phosphopantetheine adenylyltransferase (PPAT) then catalyzes the transfer of an adenylyl group from ATP to form 3′-dephospho-CoA, which is finally phosphorylated by dephospho-CoA kinase (DPCK) to generate CoA. In contrast, in higher eukaryotes the final two steps are performed by a single bifunctional enzyme named CoA synthase (Suzuki *et al.*, 1967; Worrall & Tubbs, 1983).

The unique properties of bacterial PPAT and DPCK compared with eukaryotic CoA synthase highlight the potential for these bacterial enzymes as novel targets in treating drug-resistant bacteria. This is particularly relevant for *Mycobacterium tuberculosis*, a notorious pathogen whose increasing resistance to antibiotics makes it a major worldwide health threat (Turett *et al.*, 1995; Pablos-Mendez *et al.*, 1996; Park *et al.*, 1996). Determining the structure of these tuberculin CoA biosynthetic enzymes is therefore of paramount importance and could form the foundation for structure-based design of new antibiotics. Indeed, potent peptide inhibitors have recently been described for *Escherichia coli* PPAT (Zhao *et al.*, 2003) and these might also be effective inhibitors of tuberculin PPAT.

The reaction catalyzed by PPAT is the only reversible reaction in the CoA biosynthesis pathway and this reaction is rate-limiting (Jackowski & Rock, 1984). *E. coli* PPAT is a hexamer, with the protomers having a polypeptide chain of 161 amino acids and a molecular weight of 18.7 kDa. The structure of coliform PPAT has been determined in complex with its substrates (Izard, 2002), product (Izard & Geerlof, 1999) and feedback inhibitor (Izard, 2003). *Helicobacter pylori* PPAT crystallization has also been reported (Eom *et al.*, 2003). Here, we describe the crystallization of *M. tuberculosis* PPAT, with the crystals being of sufficient quality for determination of its structure.

2. Methods and results

M. tuberculosis PPAT was expressed using the pET3 expression plasmid in *E. coli* BL21(DE3) and induced by IPTG for 6 h at 310 K. Cells were lysed in Tris–HCl pH 8, 0.5 *M* NaCl and PMSF. The protein was then purified to homogeneity by column chromatography as described for *E. coli* PPAT (Geerlof *et al.*, 1999). The purified enzyme was dialyzed into 10 m*M* Tris buffer pH 8 containing 0.5 m*M* DTT, concentrated to 18 mg ml^{-1} and aliquoted and stored at 253 K.

Initial crystallization conditions for native tuberculin PPAT were identified using the microbatch system at the Hauptman–Woodward Institute (Buffalo, NY, USA). Crystals

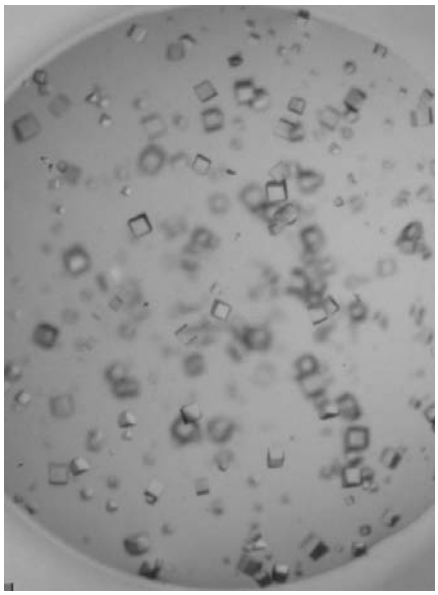

Figure 1
Crystals of tuberculin phosphopantetheine adenylyltransferase.

Table 1
Data-reduction statistics of tuberculin PPAT data set.

(*a*) Data-reduction statistics.

No. observations	441799
No. unique reflections	15683
Redundancy	28.2
$F^2 > 3\sigma(F^2)$ (100–1.95 Å) (%)	94.9
$F^2 > 3\sigma(F^2)$ (2.02–1.95 Å) (%)	75.6
Average $F^2/\sigma(F^2)$	44.9

(*b*) Completeness and $R_{\rm merge}$ in resolution shells.

Resolution range (Å)	$R_{\rm merge}$†	Completeness (%)
100.00–4.20	0.044	99.4
4.20–3.33	0.061	99.9
3.33–2.91	0.057	100.0
2.91–2.65	0.080	100.0
2.65–2.46	0.076	100.0
2.46–2.31	0.087	100.0
2.31–2.20	0.294	100.0
2.20–2.10	0.119	99.9
2.10–2.02	0.350	98.7
2.02–1.95	0.235	87.9
99.00–1.95	0.069	98.6

† $R_{\rm merge} = \sum_{\rm unique\ reflections}(\sum_{i=1}^{N} |I_i - \bar{I}|)/\sum_{\rm unique\ reflections}(\sum_{i=1}^{N} I_i)$.

appeared under oil within 1 d from the Hampton Research Nucleic Acid Mini Screen condition No. 1. Subsequent crystallization experiments were performed at room temperature using the hanging-drop vapor-diffusion technique. Crystals of tuberculin PPAT were obtained from 10% 2-methyl-2,4-pentanediol (MPD), 40 m*M* sodium cacodylate buffer pH 5.5, 20 m*M* cobalt hexamine and 20 m*M* magnesium chloride. Initial crystallization droplets of 1 µl protein solution added to 1 µl of reservoir solution resulted in PPAT crystals of dimensions of up to 0.1 mm (Fig. 1). These crystals grow overnight and their size does not increase with time. Tuberculin PPAT crystals were cryoprotected by including 35% MPD in the mother liquor.

X-ray data were collected at 100 K using a DIP2030 area-detector system (MacScience) mounted on a Nonius FR591 X-ray generator operating at 45 kV and 90 mA and equipped with focusing mirrors (MacScience). The data were processed using *DENZO* and *SCALEPACK* (Otwinowski & Minor, 1997). The data were collected at a crystal-to-detector distance of 150 mm, using 0.5° oscillations per image and an exposure time of 20 min per frame. Data statistics are provided in Table 1.

The results of autoindexing with *DENZO* (Otwinowski & Minor, 1997) are consistent with the crystals having a primitive rhombohedral lattice, with unit-cell parameters a = 68.69 Å, α = 91.81° in the rhombohedral setting (equivalent to $a = b$ = 98.48, c = 115.15 Å in the hexagonal setting). Analysis of the simulated *hk*0 precession photographs showed 6*mm* symmetry with the mirror planes every 60° about *c**, indicating the presence of twofold axes perpendicular to and related by a threefold axis. Since the dyads lie normal to the mirror plane, the tuberculin PPAT crystals belong to space group *R*32. Moreover, the $R_{\rm merge}$ for data reduced in *R*32 was not of lesser quality than for data reduced in *R*3.

The self-rotation function calculated with either the program *GLRF* (Tong & Rossmann, 1990) or *POLARRFN* (Collaborative Computational Project, Number 4, 1994) showed no significant peaks above the noise level and therefore there is no indication of a non-crystallographic twofold axis. An assumption of two protomers per asymmetric unit leads to an acceptable packing density $V_{\rm M}$ (Matthews, 1968) of 2.88 Å^3 Da^{-1}, corresponding to a solvent content of about 0.57.

We are indebted to Philippe Bois for preparing the tuberculin PPAT expression construct. We are grateful to John Cleveland for helpful comments. We thank Christina Rush, Bob Borgon and Jason Hurlbert for excellent technical assistance, Charles Ross for maintaining the X-ray and computing facilities, and Nancy Fehrman and George DeTitta for defining the initial crystallization conditions. The authors are members of the TB Structural Genomics Consortium (http://www.tbgenomics.org). This work was supported in part by the National Institutes of Health grant AI55894, the Cancer Center Support (CORE) Grant and by the American Lebanese–Syrian Associated Charities (ALSAC).

References

Abkido, Y. (1967). *Biochemistry*, **61**, 290–299.
Collaborative Computational Project, Number 4 (1994). *Acta Cryst.* D**50**, 760–763.
Eom, S. J., Ahn, H. J., Kim, H. W., Baek, S.-H. & Suh, S. W. (2003). *Acta Cryst.* D**59**, 561–562.
Geerlof, A., Lewendon, A. & Shaw, W. V. (1999). *J. Biol. Chem.* **274**, 27105–27111.
Izard, T. (2002). *J. Mol. Biol.* **315**, 487–495.
Izard, T. (2003). *J. Bacteriol.* **185**, 4074–4080.
Izard, T. & Geerlof, A. (1999). *EMBO J.* **18**, 2021–2030.
Jackowski, S. & Rock, C. (1984). *J. Bacteriol.* **158**, 115–120.
Matthews, B. W. (1968). *J. Mol. Biol.* **33**, 491–497.
Otwinowski, Z. & Minor, W. (1997). *Methods Enzymol.* **276**, 307–326.
Pablos-Mendez, A., Sterling, T. R. & Frieden, T. R. (1996). *JAMA*, **276**, 1223–1228.
Park, M. M., Davis, A. L., Schluger, N. W., Cohen, H. & Rom, W. N. (1996). *Am. J. Respir. Crit. Care Med.* **153**, 317–324.
Robinshaw, J. D. & Neely, J. R. (1985). *Am. J. Physiol.* **248**, E1–E9.
Suzuki, T., Abiko, Y. & Shimizu, M. (1967). *J. Biochem.* **62**, 542–649.
Tong, L. & Rossmann, M. G. (1990). *Acta Cryst.* A**46**, 783–792.
Turett, G. S., Telzak, E. E., Torian, L. V., Blum, S., Alland, D., Weisfuse, I. & Fazal, B. A. (1995). *Clin. Infect. Dis.* **21**, 1238–1244.
Worrall, D. M. & Tubbs, P. K. (1983). *Biochem. J.* **215**, 153–157.
Zhao, L., Allanson, N. M., Thomson, S. P., Maclean, J. K. F., Barker, J. J., Primrose, W. U., Tyler, P. D. & Lewendon, A. (2003). *Eur. J. Med. Chem.* **38**, 345–349.